7-21-2016

Enthalpy-based System-Model for Pumped Two-phase Cooling Systems

Leitao Chen
Watson Research Center, chenl12@erau.edu

Fanghao Yang
Watson Research Center

Pritish R. Parida
Watson Research Center

Mark Schultz
Watson Research Center

Timothy Chainer
Watson Research Center

Enthalpy-based System-Model for Pumped Two-phase Cooling Systems

Leitao Chen, Fanghao Yang, Pritish R. Parida, Mark Schultz, Timothy Chainer

IBM T. J. Watson Research Center, Yorktown Heights, NY, USA, 10598
Email: yangf@us.ibm.com

ABSTRACT

The development of embedded chip cooling for 2D and 3D integrated circuits using pumped dielectric refrigerant has gained recent attention due to the ability to manage high heat densities and compatibility with electronics. Recent studies have focused on in-situ thermal and hydrodynamic phenomena (e.g. boiling and bubble dynamics) of two-phase flow boiling at micro-scales. In this paper we focus on the two-phase cooling system design including the cooling capability, size and coefficient of performance (COP). In implementing a two-phase cooling, a system-level computational model for two-phase cooling systems becomes necessary. Therefore, a computationally manageable and accurate one dimensional (1D) system model is described. Furthermore, the model can be easily customized for different two-phase cooling system configurations. By validating the model with experimental data from a two-phase cooling system, it is shown that model can generate accurate results, and therefore, can be used as a tool to study and predict the characteristics and performance of a pumped two-phase cooling systems.

KEY WORDS: System model, Two-phase cooling, enthalpy

NOMENCLATURE

a	first parameter in Eq. (8)
f	friction factor
g	gravitational acceleration constant, 9.8m/s^2
h	enthalpy, J/kg
hf	heat flux, W/m^2
n	second parameter in Eq. (8)
x	vapor quality
P	pressure, Pa
z	the length in the flow direction, m
C	the C value for Lockhart-Martinelli model
D	hydrodynamic diameter, m
H	height, m
G	mass flux, kg/(m^{2}s)
T	temperature, K
X_{tt}	Martinelli parameter

Greek symbols

α	void fraction
ρ	density (kg/m^3)
θ	angle (rad)
ϕ	amplifier
μ	dynamic viscosity (Pa-s)

Subscripts

amb	ambient
fr	frictional force
g	gravitational force
i	index number for nodes during discretization
in	inlet
out	outlet
l	liquid
mo	momentum change
lc	liquid column
r	reservoir
v	vapor
sat	saturation
I	index number for segments during discretization

INTRODUCTION

The significance of cooling technologies has increasingly grown in the IT industry. The demand to increase system performance has driven the development of three-dimensional (3D) chip stacking which reduces the distance of chip communications and increases bandwidth [1, 2]. However, the 3D stacking structure can cause dramatic rises of both volumetric heat generation and heat flux in the stack, which can be over 1 kW/cm^3 and 1 kW/cm^2, respectively [3-5]. Traditional thermal solutions such as air cooling and single-phase liquid cooling have been proved insufficient due to their limited heat transfer coefficients (HTC) [6-7] and/or high pressure drop at required flow rates. Therefore, more sufficient cooling scheme is demanded. In addition, with the rapid growth of the IT sector, its energy consumption is also skyrocketing. Among the total energy consumed by IT devices, the energy for cooling is a major contributor. Recent studies for Data centers have shown that their power usage accounts for 2% of total US power consumption, of which 25%-30% is utilized by cooling [8]. To reduce the cooling power consumption, a more efficient cooling technology is required. Two-phase liquid cooling which combines excellent thermal performance and energy efficiency offers a solution to next-generation cooling technology in IT industry [9-10]. In two phase cooling heat is absorbed during the change in phase of the coolant from liquid to vapor which can sustain large heat transfer coefficients. As a result, the flow rate of the refrigerant in two-phase cooling systems can be lowered, thus decreasing pumping power consumption.

Most of current studies about two-phase cooling focused on the microscopic level, on which different geometries and configurations of flow boiling are investigated in order to estimate their effects on hydrodynamic and thermal performances, such as pressure drop, HTC and critical heat flux (CHF). For example, straight [11-13] and circular [14-16] multi microchannels have been studied both experimentally and numerically and recently, pin-fin arrays [17-18] and radial hierarchical channels [19] have been investigated due to their better temperature uniformity. However, the study of two-phase cooling at the system level is also important as microchannel evaporators require a closed loop system whose design will affect the cooling performance and energy efficiency.

Therefore, in order to understand the two-phase cooling on the system level, a system model is critical.

The system models basically serve two purposes: to improve the system design, a hardware aspect and to optimize the system control, a software aspect. Due to the fact that the development of two-phase cooling for electronics is still at its infancy, the system hardware design is more critical at the current stage. Therefore, a system model that is general in nature is highly desired. Such a generality should allow different system configurations, the addition or deletion of different types and subcomponents, and the application of different types of refrigerants, which are altogether called the front-end generality. The model should also have the back-end generality, with which one can easily replace and modify the physical models, numerical algorithms and parameters for each subcomponent in the system model to achieve a desired level of accuracy, because a good accuracy is important but usually hard to obtain for two-phase simulations due to the complexity of physics. Among a handful system models of the two-phase cooling for electronics, there is no one that can satisfy the front-end and back-end generality in the same time. For example, the models developed by Catano et al. [20, 21] and Li and Alleyne [22] adopted a lumped-variable approach. Such an approach can compute very fast, and therefore can be used to perform real-time simulations to study the control strategies. However, the back-end generality is lost due to the lack of dimensions in the model. As a result, such a model cannot be utilized to improve the system design due to its poor accuracy.

A two-phase cooling system model was developed and is described in this paper. The system model developed in this paper has the capability to customize the system by integrating different evaporators, condensers and subcomponents. It also allows building different system configurations and choice of refrigerants. The paper is organized in the following order: First, general features of the system model are described. Second, detailed numerical methods of the model are presented. Third, models of some key subcomponents in the system are discussed as well as the system model. Last, the solutions of model are compared with experimental data from an experimental system using R1234ze refrigerant.

MODEL OVERVIEW

The system-level model described in this paper has four key features that are expanded in the following four subsections.

I. Governing Equations

The model is a hybrid based upon conservation laws. The basic goal of the two-phase cooling system model is to calculate the macroscopic variables, namely the pressure (p), temperature (T) and vapor quality (x), at any location in the system. There are many approaches to calculate these variables, however, in order to achieve generality as well as accuracy, the model in this paper is constructed by solving the general one-dimensional (1D) conservation equations of mass, momentum and energy. Usually when operating a cooling system, the mass flow rate is a controllable variable. Therefore, in the system model, the mass flow rate is assumed to be a known parameter which is used to calculate other unknowns. As a result, the conservation of mass is automatically satisfied when the same mass flow rate is applied to every component in the system. Nevertheless, solving of momentum and energy conservations cannot be avoided. Solving momentum conservation equation is theoretically equivalent to calculating the pressure drop Δp, which provides a solution to p; and the solution of energy conservation equation yields T and x. The process of calculating p, T and x will be discussed in detail in the next section.

One of the key feature of the system-level model is rapid turn-around time for each simulation. However, for some system components such as a microchannel evaporator with complicated flow networks [18, 19, 23], solving the conservation equations of momentum and energy turns out to be computationally intensive (in a relative manner). Therefore, higher-level abstractions in the form of correlations or characteristic curves based on experimental data is chosen to obtain the values of p, T and x, instead of solving the conservation equations resulting in a hybrid model. Additionally, the REFPROP software [24] was used for computing the various fluid intrinsic properties. The calculations of the thermodynamic and transport properties of the refrigerant can be very accurate due to the high-fidelity equations of state (EOS) in the REFPROP library [24].

II. Model Generalization and Modularity

In order to create a general model that has the maximum flexibility to simulate systems with different configurations, design and operating conditions, the system model (illustrated in Figure 1) is entirely modularized with Object-Oriented Programming (OOP) and is integral to each component of the system model (Figure 2). For any component in the system, such as pipe, pump or condenser, etc., its model can be generalized as a black box, which has inputs P_{in}, T_{in} and x_{in} and generates the output P_{out}, T_{out} and x_{out} according to the characteristics of the component.

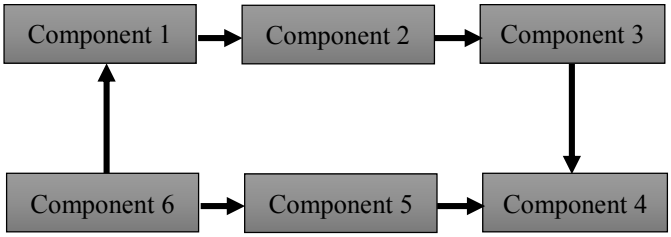

Fig. 1 General system model

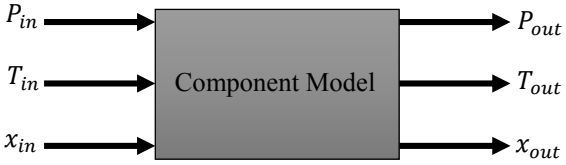

Fig. 2. General component model

In addition, each component model can fully work on its own and is self-contained. It has full functionality to calculate its own output variables based on its input, regardless of which other component model it is connected. This allows each component model to be repeatedly used, which dramatically reduces the effort to reuse, maintain and develop the models. Each component model has its own algorithm to calculate its

output variables. Since each component model itself is also modularized, the modification or replacement of such an algorithm does not affect other factors of the component model, such as the size and material property. Therefore, the methodology to generate output variables could be an algorithm that solves the momentum and energy conservation equation, such as for a pipe or condenser, or a *P-V* curve or other characteristic curves or even experimental data that can replace solving of momentum conservation, such as for the pump. This feature is extremely important because it allows the components with different natures to be plugged into the system without any significant changes to the system model.

III. Numerical Model - Enthalpy Conservation

The numerical model is the core of this system model, which is enclosed in each component model to calculate its P_{out}, T_{out} and x_{out} as shown in Figure 2. The numerical model is the solver of each component model and also the entire system model. The model requires that P_{in}, T_{in} and x_{in} be known or obtainable. The exact form of numerical model may vary from component to component, however, they all have the same basic structure.

For a two-phase system, phase change occurs inevitably with energy transfer. Regardless of whether the flow is single-phase or two-phase, or whether phase change happens or not, the total enthalpy is conserved. The energy conservation in the form of enthalpy equation is shown in Eq. (1). For any component in the system, h_{in} is known either as an output from preceding component or as a starting assumption and Δh is also known since it is the total energy added or subtracted into or from the component, including the small amount of heat exchange with the environment. Therefore, h_{out} can be calculated by Eq. (1). In order to define the thermodynamic state of the coolant, another thermodynamic property is required. For the present study, we chose that to be P_{out} which is calculated by using Eg (2). Using these two properties as component outputs, T_{out} and x_{out} can be calculated. Similarly, to the enthalpy calculation, for any component, P_{in} is known either as an output from preceding component or as a starting assumption. However, ΔP is not known and can be calculated using the process described in the following section.

$$h_{out} = h_{in} + \Delta h \tag{1}$$

$$P_{out} = P_{in} + \Delta P \tag{2}$$

IV. Numerical Model – Pressure Drop Calculation

The pressure drop, across a system component can be obtained in different ways. Usually, for any components in the flow system, the pressure difference ΔP (the pressure after the component minus its inlet pressure) can be characterized in term of flow rate. For a pump, which is the flow motivator, ΔP is positive; for all other components in the system such as pipes, valves and the testing device, which have a flow resistance, ΔP is negative. Such a characteristic of a certain component is called the *P-V* curve, which is usually acquired from experiments. For some components like pumps and flowmeters, their *P-V* curves are available through product literature while others can be obtained experimentally. For such cases, ΔP can simply be interpolated from these curves.

However, for other components like pipes, the approach of using a *P-V* curve becomes more difficult. There are two reasons. First, the piping in a flow system is variable with different length, number of bends and altitude (relative height differences). It would be very tedious to characterize the *P-V* curve with experiments for each pipe section; secondly, the flow in each pipe could be single-phase with different temperatures or two-phase with different flow regimes, so the full characterization of each pipe would require not just one curve but many, which is nearly impractical. Consequently, a more fundamental model becomes necessary, which is the conservation equation of momentum. By building the momentum conservation equation for general flows (single-phase or two-phase) and performing some transformations [25], we obtain the equation shown below.

$$-\left(\frac{dP}{dz}\right)_{total} = \left(\frac{dP}{dz}\right)_{fr} + \left(\frac{dP}{dz}\right)_{g} + \left(\frac{dP}{dz}\right)_{mo} \tag{3}$$

Per equation (3), the total pressure gradient along the flow direction $\boldsymbol{z}$ has three contributors: the frictional force, the gravitational force and the change of momentum due to acceleration or deceleration. In Eq. (3),

$$\left(\frac{dP}{dz}\right)_{g} = [(1-\alpha)\rho_l + \alpha\rho_v]g \cdot sin\theta \tag{4}$$

$$\left(\frac{dP}{dz}\right)_{mo} = \frac{d}{dz}\left[\frac{G^2x^2}{\rho_v\alpha} + \frac{G^2(1-x)^2}{\rho_l(1-\alpha)}\right] \tag{5}$$

Equations (3)-(5) are valid only with a few assumptions. First, the cross-section of the flow has the same area along the flow direction; second, the velocities of liquid and vapor phases may be different, but within each phase the velocity is uniform; third, both two phases are in local thermodynamic equilibrium. All pressure drop (force) contributors have their explicit forms for evaluation except that for the frictional force. The reason is that there is no accurate theoretical model for frictional pressure gradient, however there are numerous correlation models. The merit about this numerical model is that the users can choose different correlation models for frictional pressure gradient or even incorporate their own. The correlation used in this paper is Lockhart-Martinelli [26], which is described by means of the following equations.

$$\left(\frac{dP}{dz}\right)_{fr} = -\phi_l^2\left(\frac{dP}{dz}\right)_{l} \tag{6}$$

where

$$\left(\frac{dP}{dz}\right)_{l} = -\frac{2f_lG^2(1-x)^2}{\rho_lD} \tag{7}$$

where the liquid friction factor f_l has the following form:

$$f_l = a\left(\frac{G(1-x)D}{\mu_l}\right)^n \tag{8}$$

in which a and n will take different values for different flow regimes. For laminar flows, $a = 16, n = 1$; for turbulent flows, $a = 0.079, n = 0.25$. In Eq. (6), ϕ_l^2 is the multiplier that has the following form:

$$\phi_l^2 = 1 + \frac{C}{X_{tt}} + \frac{1}{X_{tt}^2} \tag{9}$$

Where C is determined by the flow regimes of both liquid and vapor phases, which is listed in the following table.

Table 1. C value for Lockhart-Martinelli model

Liquid	Vapor	C
Turbulent	Turbulent	20
Laminar	Turbulent	12
Turbulent	Laminar	10
Laminar	Laminar	5

In Eq. (9), X_{tt} is the Martinelli parameter that is calculated in the following equation:

$$X_{tt} = \left(\frac{1-x}{x}\right)^{0.9} \left(\frac{\rho_v}{\rho_l}\right)^{0.5} \left(\frac{\mu_l}{\mu_v}\right)^{0.1} \tag{10}$$

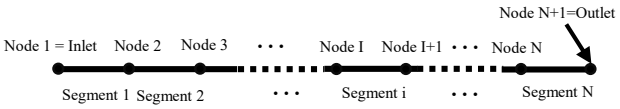

Fig. 3 Discretization of the flow channel

Using equations (3)-(10), the total pressure gradient can be calculated. However, in order to calculate the pressure drop, it is necessary to take the integral of the pressure gradient over the length of the flow channel. Here, it is chosen to calculate the numerical integral by discretizing the flow channel into segments with equal spacing, such as that in Figure 3. The flow channel is divided into N segments with equal spacing Δz, with e $N+1$ nodes, where node 1 is the inlet and node $N+1$ is the outlet. In segment i in Figure 3, for frictional and gravitational forces, their pressure gradients at two terminal nodes I and $I+1$ are calculated first, as follows.

$$\begin{cases} \left(\frac{dP}{dz}\right)_{fr,I} = -\phi_{l,I}^2 \left(\frac{dP}{dz}\right)_{l,I} \\ \left(\frac{dP}{dz}\right)_{fr,I+1} = -\phi_{l,I}^2 \left(\frac{dP}{dz}\right)_{l,I+1} \end{cases} \tag{11}$$

$$\begin{cases} \left(\frac{dP}{dz}\right)_{g,I} = \left[(1-\alpha_I)\rho_{l,I} + \alpha_I \rho_{v,I}\right] g \cdot sin\theta \\ \left(\frac{dP}{dz}\right)_{g,I+1} = \left[(1-\alpha_{I+1})\rho_{l,I+1} + \alpha_{I+1} \rho_{v,I+1}\right] g \cdot sin\theta \end{cases} \tag{12}$$

Then, a simple average is taken between two terminal nodes in the following equations, which are the pressure gradients in segment i.

$$\left(\frac{dP}{dz}\right)_{fr,i} = \left[\left(\frac{dP}{dz}\right)_{fr,I} + \left(\frac{dP}{dz}\right)_{fr,I+1}\right]/2 \tag{13}$$

$$\left(\frac{dP}{dz}\right)_{g,i} = \left[\left(\frac{dP}{dz}\right)_{g,I} + \left(\frac{dP}{dz}\right)_{g,I+1}\right]/2 \tag{14}$$

So, the pressure drops due to frictional and gravitational forces in segment i are

$$(\Delta P)_{fr,i} = \left(\frac{dP}{dz}\right)_{fr,i} \Delta z = \Delta z \left[\left(\frac{dP}{dz}\right)_{fr,I} + \left(\frac{dP}{dz}\right)_{fr,I+1}\right]/2 \tag{15}$$

$$(\Delta P)_{g,i} = \left(\frac{dP}{dz}\right)_{g,i} \Delta z = \Delta z \left[\left(\frac{dP}{dz}\right)_{g,I} + \left(\frac{dP}{dz}\right)_{g,I+1}\right]/2 \tag{16}$$

By doing this on each segment and summing them together, the pressure drops due to frictional and gravitational forces along the entire flow channel are

$$(\Delta P)_{fr} = \sum_1^N (\Delta P)_{fr,i} \tag{17}$$

$$(\Delta P)_g = \sum_1^N (\Delta P)_{g,i} \tag{18}$$

For the third contributor of pressure gradient, the change of momentum, it could also be calculated like the other two. But because all internal terms will be canceled out with only the first and last terms left, the pressure drop due to momentum change is shown as follows.

$$(\Delta P)_{mo} = \left[\frac{G^2 x^2}{\rho_v \alpha} + \frac{G^2 (1-x)^2}{\rho_l (1-\alpha)}\right]_{out} - \left[\frac{G^2 x^2}{\rho_v \alpha} + \frac{G^2 (1-x)^2}{\rho_l (1-\alpha)}\right]_{in} \tag{19}$$

As a result, the total pressure along the flow channel is

$$-(\Delta P)_{total} = (\Delta P)_{fr} + (\Delta P)_g + (\Delta P)_{mo} \tag{20}$$

It is worth noting that all variables are changing along the flow direction. Therefore, those variables have to be calculated at each node of the discretized flow channel separately. Among those variables, the vapor quality x dramatically affects the pressure drop. Therefore, it is necessary to identify the impactors that would change x and then calculate x at each node. Primarily there are two impactors: external heat and pressure. However, since external heat has greater impact on the change of x than pressure, it is assumed in this paper that external heat is the only contributor to x along the flow direction. Therefore, in order to calculate the total pressure drop, it is required to calculate the profile of vapor quality along the flow channel with known external heat profile. In Figure 3 again, the external heat profile, which is defined by the user, identifies the heat flux at each node. So, taking segment i for example, the heat flux is given by

$$hf_i = [hf_I + hf_{I+1}]/2 \tag{21}$$

By using the energy conservation within segment i and the known conditions at node I, the vapor quality at node $I+1$ can be calculated. By doing this sequentially from left to right for each segment, the vapor quality at each node can be determined. It is worth noting that the calculation for the last segment will generate the vapor quality at the outlet x_{out}. However, this value is only used to calculate the pressure drop in the last segment. And the real x_{out} is obtained using h_{out}, P_{out} and equations of state. It can be easily concluded that, for a special case, in which the external heat is zero, the vapor quality does not change along the flow direction. However, x_{out} may be different from x_{in} due to change in state of the coolant from inlet to outlet.

SYSTEM MODEL AND KEY COMPONENTS

The actual system may vary in terms of the type and number of components in the system. Some component may be necessary in one system but absent in another. So, in this section, we will discuss components that are necessary in most system configurations.

Pump

The pump P-V curve can give the pressure head, a positive ΔP, under different flow rate. This is then used in Eq. (2) to calculate the pressure at outlet. Lastly, the equations of state are then used to calculate the temperature and vapor quality at the outlet of the pump.

Pipe

First, it should be determined that how much heat the pipe is exchanging with the environment, which is typically very small. Secondly, a profile for the heat exchange along the pipe is assumed. Commonly, a uniform profile is assumed. Lastly, the full functionality described in sections III and IV above are used to calculate P_{out}, T_{out} and x_{out} of the pipe.

Condenser

The condenser model is a half full physical model, in which the split is taken at the heat transfer between the refrigerant coolant and ambient environment. The temperature of the ambient environment is assumed as a constant value. The heat would be simply rejected into ambient environment. Therefore, the condenser is simplified as a special pipe for this study.

Reservoir

The reservoir plays an import role in the system with several functionalities. First, it dampens the oscillation of the flow and therefore stabilizes the system. Second, it always provides subcooled flow at its outlet by creating a liquid column within its container. Since the reservoir introduces some discontinuity between its inlet and outlet, its numerical model is slightly different from others. First, the pressure at its outlet is calculated with the following equation

$$P_{out} = \frac{1}{2}P_{in} + \frac{1}{2}P_r + \Delta P_{lc} \tag{22}$$

where P_r is the static pressure inside of the reservoir and ΔP_{lc} is the pressure head due to the liquid column.

It is assumed that the fluid inside of the reservoir is always saturated and thus, P_r is equal to its saturation pressure. Then, if the corresponding saturation temperature is known, P_r can be obtained using the coolant's saturation properties. It is assumed that the temperature inside of the reservoir is equally influenced by the ambient temperature and the temperature of the reservoir inlet given by;

$$T_r = \frac{1}{2}T_{amb} + \frac{1}{2}T_{in} \tag{23}$$

The pressure head due to liquid column is computed with the following equation.

$$\Delta P_{lc} = \rho_l g H \tag{24}$$

where the height of the liquid column H is known and should be a constant value for steady-state model.

Once the outlet pressure is available, equations of state are used to calculate T_{out} and x_{out}.

Testing Section / Micro-evaporator

The test section is a micro-evaporator where the most complicated physics occurs. The refrigerant evaporates and cools down the electronic device (e.g. CPU). The reason why it is complicated is because the geometry of the flow passages are micron scale and include complex geometries such as pin fin arrays. Solving the conservation equations is very computationally expensive [27]. Although, recent studies have demonstrated reduced order models [28-29] to evaluate heat transfer and pressure drop in micro-channels based micro-evaporators, the models are currently not applicable to the test-section studied here. For the present study, it was chosen to build a correlation between pressure drop and flowrate and heat generation with experiments. As a result, the pressure drop can be interpolated at each given flow rate and heat generation from the device under test. Once P_{out} and h_{out} are known, T_{out} and x_{out} can be calculated using the equations of state.

The System

Once each component model is complete, the system model can be built by connecting each component model according to the system configuration. The steady-state solution is achieved iteratively. First the values for p, T and x at the inlet or outlet of a given component is assumed. Next, the computation on components one by one along the flow direction is carried out. Once the full circle is reached, the new values of p, T and x are compared to the values from the previous iteration. If the differences are within a defined tolerance, the solution has converged; otherwise, iteration continues.

TEST RESULTS AND DISCUSSIONS

The system model was validated by comparing its simulation results with those from an experimental setup that was built to measure local temperature in radial microchannels with pin arrays in a previous study [19, 30]. A schematic of this setup is shown in Figure 4. This setup is a closed loop flow system, which comprises a micro test device referred to as thermal test vehicle (TTV), a reservoir, a condenser, a magnetic drive gear pump and a Coriolis mass flowmeter. The thermal test vehicle sits on a test board, which provides all electrical and signal connections. Pressures in the loop were monitored by three pressure transducers with 0.25% accuracy. To measure the fluid inlet and outlet temperatures, K-type thermocouples (TCs) were attached onto the inlet and outlet tubing, very close to the test vehicle. These tubing mounted TCs showed a temperature difference of up to 0.3 °C relative to immersed T-type TCs. Those K-type TCs shall have a combined accuracy better than 0.6 °C.

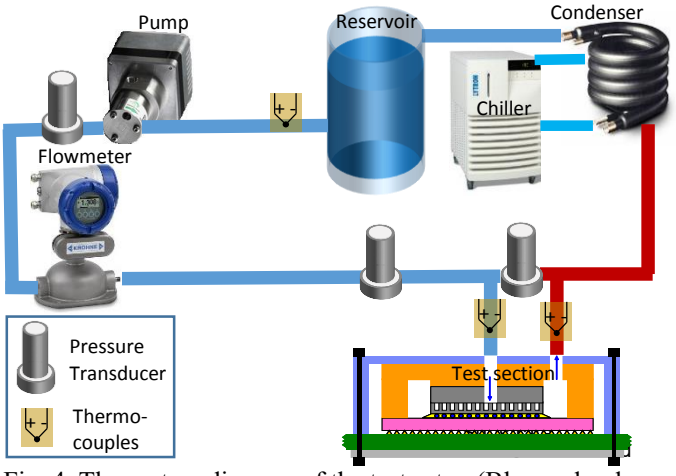

Fig. 4. The system diagram of the test setup (Blue and red wires represent flow tubing)

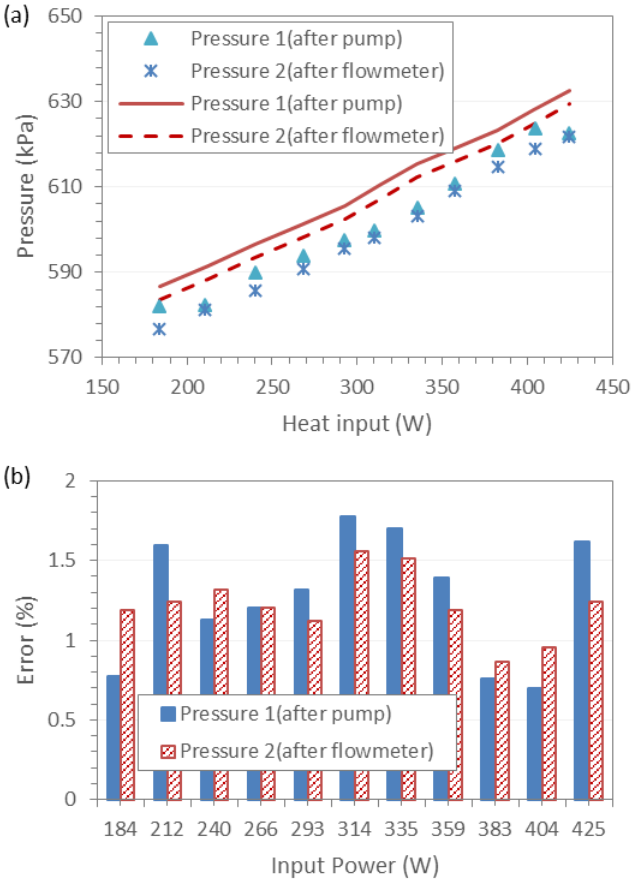

Fig. 5 (a) Pressure as a function of heat input in the test vehicle (dots are experimental data and lines are modeling results). (b) The percentage errors of pressures. Flow rate is 15 kg/hr.

The temperature of the condenser was controlled by a recirculating chiller set at 18 °C. This is the temperature of the liquid on the chiller side. The refrigerant temperature at the condenser outlet (system-side) is tightly coupled to the chiller temperature and is usually 1 – 2 °C higher due to the thermal resistance across the condenser coils. In this study, to simulate a cooling system with the highest coefficient of performance (COP), the inlet sub-cooling was not controlled as the pre-heater that could be used for such control would consume extra energy. The total mass flow rate was actively controlled by a PID (proportional-integral-derivative) algorithm driving the pump to maintain a constant flow rate using the mass-flow meter's measurement.

In addition, the heat exchanges of all subcomponents except the test section and condenser are included. Numerically speaking, in Eq. (1), the delta h of each of those subcomponent is the heat exchange with the environment. Δh is calculated with the Newton's cooling equation, where the temperature difference is computed with an assumed constant environment temperature, the heat transfer coefficient is assumed to be $10 W/m^2 \cdot K$ for natural convection.

The test results were compared with the system model of the actual test system. The results are plotted as functions of heat input in the test vehicle, which mimics the heat generation in a micro-processer. First, the pressures at the outlets of pump and flowmeter were compared and are summarized in Figure 5. As shown the system model could predict pressures in the system with good accuracy. The errors were observed to be within a range of 9 – 12 kPa. The majority of the errors can be attributed to the correlations used for the pump and the test vehicle pressure drops. Second, refrigerant temperatures before and after the test-section were also measured and compared to the simulation results as shown in Figure 6. The figure shows that the simulation model results are in good agreement with the experimental results within 0.25 °C, which is within the measurement errors of the TCs.

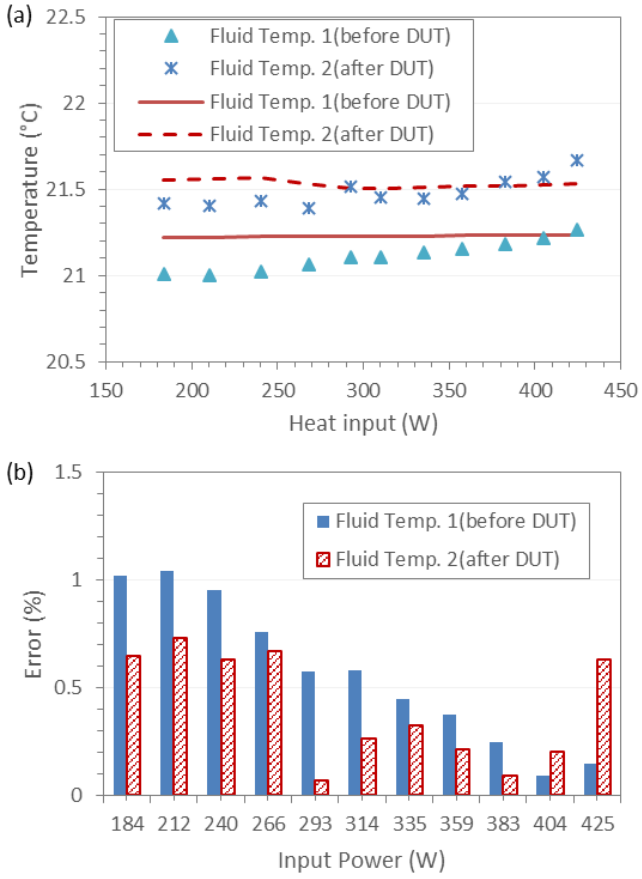

Fig. 6 (a) Fluid temperature as a function of heat input in the test vehicle (dots are experimental data and lines are modeling results). (b) The percentage errors of fluid temperatures. Flow rate is 15 kg/hr.

CONCLUSIONS

A system model for general two-phase cooling systems has been developed. Its physical models, assumptions and numerical methods have been summarized in detail. The system model was validated with an experimental two phase cooling system under different heat loading of a thermal test vehicle. The model described in this paper was able to predict the pressures and temperatures at any location in the system.

In addition, the model is not designed for a specific system, but could be customized for any pumped two-phase cooling system. Therefore, it can be utilized as a platform to study existing systems or design new systems with reliable prediction.

Acknowledgments

This project was supported in part by the U.S. Defense Advanced Research Projects Agency Microsystems Technology Office ICECool Applications Program under the award number FA8650-14-C-7466. Disclaimer: The views, opinions, and/or findings contained in this article are those of the authors and should not be interpreted as representing the official views or policies of the Department of Defense or the U.S. Government.

The authors would like to thank other team members from IBM Research involved in the ICECool program for their valuable technical contributions and discussions. The author would like to thank Avram Bar-Cohen and Kaiser Matin from DARPA for their technical support and project guidance.

References

[1]. C. R. King, Jr., D. Sekar, M. S. Bakir, B. Dang, J. Pikarsky, and J. D. Meindl, "3D Stacking of Chips with Electrical and Microfluidic I/O Interconnects," Electronic Components and Technology conference, 2008.

[2]. B. Dang, M. S. Bakir, D. C. Sekar, C. R. King, Jr., and J. D. Meindl, "Integrated Microfluidic Cooling and Interconnects for 2D and 3D chips," IEEE Transactions on Advanced Packaging, vol. 33. no. 1, pp. 79-87, Feb. 2010.

[3]. Marcinichen, J., Brian P., Thome, J., Lewis, J., and Venkatasubramaniam, R., "Thermal management of ultra intense hotspots with two-phase multi-microchannels and embedded thermoelectric cooling", Proceedings of the ASME 2013 international technical conference and exhibition on packaging and integration of electronic and photonics microsystems, 2013.

[4]. DARPA BAA 12-50, "Intrachip/interchip Enhanced Cooling (ICECool) Fundamentals" June 2012.

[5]. DARPA BAA 13-21, "Intrachip/interchip Enhanced Cooling (ICECool) Applications", Feb 2013.

[6]. D. B. Tuckerman, and R. F. W. Pease, "High-performance heat sinking for VLSI," IEEE Electron Device Letters, vol. 5, pp. 126-129, 1981.

[7]. T. Brunschwiler, S. Paredes, U. Drechsler, B. Michel, W. Cesar, Y. Leblebici, B. Wunderle, and H. Reichl, "Heat-removal performance scaling of interlayer cooled chip stacks," In Thermal and thermomechanical phenomena in electronic system (ITerm), 12th IEEE Intersociety Conference,2010.

[8]. Koomey, J.G., 2011, "Growth in Data Center Electricity Use 2005 to 2010", Oakland, CA: Analytics Press.

[9]. Kandlikar, S. G., "History, Advances, and Challenges in Liquid Flow and Flow Boiling Heat Transfer in Microchannels: A Critical Review," J. Heat Transf.-Trans. ASME, 134(3), 2012.

[10]. J. Marcinichen, J. Olivier, and J. R. Thome, "Reasons to use two-phase refrigerant cooling," Electronics Cooling, 2011.

[11]. D. Lelea, S. Nishio, and K. Takano, "The experimental research on micro-tube heat transfer and fluid flow of distilled water," International Journal of Heat Mass transfer, vol. 47, pp. 2817-2830, 2004.

[12]. J. Lee, and I. Mudawar, "Two-phase flow in high-heat-flux micro-channel heat sink for refrigeration cooling applications: Part I - Pressure drop characteristics," International Journal of Heat Mass Rransfer, vol. 48, pp. 928-940, 2005.

[13]. S. J. Kim, and D. Kim, "Forced convection in microstructures for electronic equipment cooling," ASME Journal of Heat Transfer, vol. 121, pp. 639-645, 1999.

[14]. M. B. Bowers, and I. Mudawar, "High Flux Boiling in Low Flow Rate, Low Pressure Drop Mini-Channel and Micro-Channel Heat Sinks," Int. J. Heat Mass Transfer, vol. 37, pp. 321–332, 1994.

[15]. M. B. Bowers, and I. Mudawar, "Two-Phase Electronic Cooling Using Mini-Channel and Micro-Channel Heat Sinks—Part 1. Design Criteria and Heat Diffusion Constraints," ASME J. Electron. Packag., vol. 116, pp. 290–297, 1994.

[16]. M. B. Bowers, and I. Mudawar, "Two-Phase Electronic Cooling Using Mini-Channel and Micro-Channel Heat Sinks—Part 2. Flow Rate and Pressure Drop Constraints," ASME J. Electron. Packag., vol. 116, pp. 298–305, 1994.

[17]. T. Brunschwiler, B. Michel, H. Rothuizen, U. Kloter, B. Wunderle, H. Oppermann, and H. Reichl, "Interlayer cooling potential in vertically integrated packages," Microsystem Technologies, vol. 15, no. 1, pp. 57-74, 2009.

[18]. C. L. Ong, S. Paredes, A. Sridhar, B. Michel, and T. Brunschwiler, "Radial hierarchical microfluidic evaporative cooling for 3-D integrated microprocessors," Proceedings of the 4th European Conference on Microfluidics, 2014

[19]. Schultz, M., F. Yang, E. Colgan, R. Polastre, B. Dang, C. Tsang, M. Gaynes, P. Parida, J. Knickerbocker, T. Chainer, "Embedded Two-Phase Cooling of Large 3D Compatible Chips with Radial Channels", Proceeding of ASME InterPACK / ICNMM 2015, July 6-9, San Francisco, CA, 2015.

[20]. Juan Catano, Tiejun Zhang, John T. Wen, Michael K. Jensen and Yoav Peles, "Vapor compression refrigeration cycle for electronics cooling – Part I: Dynamic modeling and experimental validation," International Journal of Heat and Mass Transfer, vol. 66, pp. 911-921, 2013.

[21]. Juan Catano, Fernando Lizarralde, Tiejun Zhang, John T. Wen, Michael K. Jensen and Yoav Peles, "Vapor compression refrigeration cycle for electronics cooling – Part II: gain-scheduling control for critical heat flux

avoidance," International Journal of Heat and Mass Transfer, vol. 66, pp. 922-929, 2013.

[22]. Bin Li and Andrew G. Alleyne, "A dynamic model of a vapor compression cycle with shut-down and start-up operations," International Journal of Refrigeration, vol. 33, pp. 538-552, 2010.

[23]. P. R. Parida, A. Vega, A. Sridhar, T. Brunschwiler, A. Buyuktosunoglu, J. Silberman, C. Tyberg, T. Chainer, "Chip-Embedded Two Phase Cooling for Energy Efficient High Performance Computing", Workshop on Modeling & Simulation of Systems and Applications (ModSim), August 12-14, Seattle, WA, 2015.

[24]. Lemmon, E.W., Huber, M.L., McLinden, M.O, NIST Standard Reference Database 23: Reference Fluid Thermodynamic and Transport Properties-REFPROP, Version 9.1, National Institute of Standards and Technology, Standard Reference Data Program, Gaithersburg, 2013.

[25]. Van P. Carey, Liquid-Vapor Phase-Change Phenomena, 2nd Edition, New York, NY, 2008.

[26]. Lockhart, R. W., and Martinelli, R. C., "Proposed correlation of data for isothermal two-phase, two-component flow in pipes", Chem. Eng. Progress, vol. 45, no. 1, pp. 39-48, 1949.

[27]. P. R. Parida, H. Tsuei, T. J. Chainer, "Eulerian Multiphase Conjugate Model for Chip-Embedded Micro-Channel Flow Boiling", Proceeding of ASME InterPACK / ICNMM, July 6-9, San Francisco, CA, 2015.

[28]. P. R. Parida, "Reduce Order Modeling for Chip-Embedded Micro-Channel Flow Boiling", Proceeding of ASME InterPACK / ICNMM, July 6-9, San Francisco, CA, 2015.

[29]. A. Sridhar, P. R. Parida, C. Gorle, C. Lee-Ong, S. Paredes, T. Brunschwiler, B. Michel, E. Colgan, T. Chainer, K. Goodson, "Thermal Design of a Hierarchical Radially Expanding Cavity for Two-phase Cooling of Integrated Circuits", Proceeding of ASME InterPACK / ICNMM, July 6-9, San Francisco, CA, 2015.

[30]. F. Yang, M. Schultz, P. Parida, E. Colgan, R. Polastre, B. Dang, et al., "Local Measurements of Flow Boiling Heat Transfer on Hot Spots in 3D Compatible Radial Micro-channels," Proceeding of ASME InterPACK / ICNMM, July 6-9, San Francisco, CA, 2015.